Design analysis and experimental behavior of precast concrete double-tee girders prestressed with carbon-fiber-reinforced polymer strands

Saverio Spadea, Marco Rossini, and Antonio Nanni

- This paper discusses the design philosophy and the flexural performance under service loads of the precast, prestressed concrete girders made of innovative materials and novel composite manufacturing technologies for a recently constructed pedestrian bridge.
- The two girders, cast in the shape of double-tees with shortened flange overhangs, were prestressed with carbon-fiber-reinforced polymer tendons and reinforced with basalt-fiber-reinforced polymer bars.
- Carbon-fiber-reinforced polymer prestressing technology can be successfully used in thin-walled concrete sections beyond the limits suggested by current literature and without significant technological drawbacks.

Being versatile, economical, and durable (under certain conditions), reinforced concrete and prestressed concrete are the most widely used structural materials throughout the world. Unfortunately, corrosion of steel reinforcement is a major cause of durability problems in aged reinforced concrete structures.[1] In well-preserved structures, corrosion is prevented due to the alkalinity of the solution filling the concrete pores, which promotes the formation of a thin oxide layer inducing passivation of steel. However, this passivity may be lost when carbonation occurs or a critical amount of chloride ions reaches the steel surface.[2] Chloride-induced corrosion, which occurs in reinforced concrete structures exposed to seawater or deicing salts, is particularly critical because it progresses rather rapidly. Reinforced concrete durability thus depends on a sufficiently thick and dense concrete cover, the effectiveness of which is time limited and susceptible to overwhelming phenomena, such as cracking and local damage.

A strategy for ensuring the long-term durability of reinforced concrete and prestressed concrete structures is to use reinforcement that is not susceptible to corrosion. Fiber-reinforced polymers (FRPs) are a proven nonmetallic

alternative to steel that have the advantage of being highly corrosion resistant. They consist of a fibrous reinforcing component (for example, carbon, glass, aramid, or basalt fibers) embedded in a polymer matrix (for example, epoxies or vinyl esters). The fibers provide strength and stiffness to the composite and carry most of the applied load while the resin encapsulates them, thus transferring stresses and providing protection.[3] Glass is currently the most commonly used fiber for nonprestressed reinforcement, with advantages such as high strength, low cost, high chemical resistance, and insulating properties. Its drawbacks include low elastic modulus, sensitivity to abrasion and creep rupture, and low fatigue strength.

Basalt fibers have properties similar to glass fibers, but their use is quite recent. They have gained increasing attention as a reinforcing material for civil applications because their production process requires a lower amount of energy and does not require the use of additives.[4] Although basalt fiber properties can vary depending on the source of the volcanic rock they are derived from, they are attractive with respect to both cost and sustainability.[5] Carbon, more than aramid, is the preferred fiber for FRP prestressing applications due to its higher strength and lower sensitivity to creep rupture, but it is rarely used for reinforcing bars due to its high cost.

A concrete bridge completely reinforced with FRP was recently constructed for pedestrian traffic.[6,7] The bridge consists of two precast, prestressed concrete girders; two cast-in-place concrete pile caps; eight auger-cast piles; side blocks; back walls; deck topping; and curbs. The reinforcing bars comprise basalt-fiber-reinforced polymer (BFRP) with an epoxy resin matrix and glass-fiber-reinforced polymer (GFRP) with a vinyl ester resin matrix. The prestressing tendons are carbon-fiber-reinforced polymer (CFRP) with an epoxy resin. Stainless steel was used for the bearing plates of the girders, the anchor bolts for the lampposts, and the railings. New fabrication technologies, including continuous closed stirrups and preassembled pile cages, similar to that described by Spadea et al.,[8] were also employed. As a result, there is not a single pound of carbon steel in any element of the bridge.

This study deals with the design philosophy and the flexural performance under service load of the precast, prestressed concrete girders that constitute the deck of the bridge. The two girders are in the shape of double tees with shortened flange overhangs. These kinds of precast concrete elements, commonly used as floors for parking structures, are particularly thin and efficient. Their employment in a pedestrian bridge allows the construction process to be greatly simplified because it is not necessary to perform the casting in place of a separate deck but only to overlay the precast concrete elements with a concrete topping.

The double tees are reinforced with BFRP, and each stem is prestressed with nine CFRP strands with 0.6 in. (15 mm) nominal diameters. Existing applications of the CFRP prestressing technology include box beams, decked bulb-tee beams, I-beams, and double tees.[7,9–14] Nevertheless, the prestressing of CFRP tendons remains a challenge because of the high sensitivity of the material to sharp objects, which does not allow the use of tensioning systems that are conventionally used for steel strands. Previous examples of double-tee girders include a fewer number of CFRP tendons per stem (either two or three tendons). Either smaller strand diameters or thicker concrete sections were used.[7,14] Finally, the percentage of guaranteed strength applied to the CFRP tendons of the pedestrian bridge intentionally exceeds the limitation imposed by ACI 440.4R-04 guidelines[15] that appears to be overly conservative compared with recommendations issued by the Japan Society of Civil Engineers (JSCE).[16] The level of prestress in this case study has not been achieved previously in other applications featuring concrete elements with thin cross sections.

The specifications and the properties of the materials (CFRP, BFRP, and concrete), based on tests conducted either by the authors or the producers, are reported in this paper. The design philosophy of the bridge and the construction details of the double tees are presented. The construction phases of the double tees, including the monitoring of strains on instrumented CFRP strands during the different phases, are then illustrated. Finally, the results of an experimental test performed with a concentrated load corresponding to service condition are presented and discussed.

Materials

CFRP tendons

CFRP tendons are recognized as being of interest to the departments of transportation (DOTs) as corrosion-resistant reinforcing solutions.[7] CFRP strands have higher tensile fatigue resistance than steel strands and a similar relaxation ratio. CFRP creep elongation is negligible, smaller than that of other FRP materials, such as GFRP and aramid FRP, and similar to that of steel strands.

Carbon-fiber-composite cable tendons comprising seven individual wires were used in this study. Each wire consists of carbon fibers impregnated with thermosetting epoxy resin (with an average fiber–to–resin volume fraction ratio of 0.75) and protected with wrapping material (polyester fiber). The strand has a 0.6 in. (15 mm) nominal diameter and a guaranteed ultimate strength f^*_{pu} of 339 ksi (2340 MPa). According to ACI 440.1R, an environmental reduction factor C_E of 0.9 should be adopted for CFRP composites. This results in a design ultimate strength f_{pu} of 305 ksi (2106 MPa).

Table 1. Mechanical properties of carbon-fiber-reinforced polymer and steel prestressing tendons

Material	Nominal diameter, in.	Area, in.²	Breaking load, kip	Guaranteed load, kip	Yield load, kip	Elastic modulus, ksi
Carbon-fiber-composite cable (1 × 7)	0.6	0.179	83.1	60.7	n/a	21,600
Steel (1 × 7)	0.6	0.217	61.2	58.6	54.5	28,700

Note: n/a = not applicable. 1 in. = 24.5 mm; 1 kip = 4.448 kN; 1 ksi = 6.895 MPa

Table 2. Mechanical properties of basalt-fiber-reinforced polymer reinforcement

Bar type	Nominal diameter, in.	Average area, in.²	Peak load, kip	Guaranteed load, kip	Nominal ultimate strain, %	Elastic modulus, ksi
No. 3	0.375	0.151	19.7	17.4	1.32	6590
No. 4	0.5	0.244	29.3	25.8	1.70	7080
No. 8	1	0.887	98.9	81.7	1.70	6560

Note: no. 3 = 10M; no. 4 = 13M; no. 8 = 25M; 1 in. = 24.5 mm; 1 kip = 4.448 kN; 1 ksi = 6.895 MPa.

Table 1 shows the mechanical properties measured by the manufacturer on the specific production lot and the values exhibited by conventional low-relaxation steel strands that have the same nominal diameter but slightly higher cross-sectional area. A comparison between the two sets of data shows how carbon-fiber-composite cable can be considered a more efficient prestressing material than traditional high-strength steel because of its higher breaking load and lower modulus of elasticity. The high tensile strength of carbon-fiber-composite cable allows a high prestressing rate, while the lower elastic modulus reduces losses due to the elastic shortening and creep of concrete. The nominal failure capacity guaranteed by the manufacturer is 60.7 kip (270 kN), a value slightly higher than the capacity of the steel strand.

The long-term relaxation losses were measured by the manufacturer by mean of 1000 h tests conducted on CFRP tendons subjected to a strain corresponding to 0.7 f^*_{pu} under temperature conditions of 68 ± 4°F (20 ± 2°C). The following logarithmic relation[17] was extrapolated from the experimental data obtained from three different specimens using the least squares method:

$$Y = 0.147 + 0.142\log T \quad (1)$$

where

Y = relaxation rate

T = time

BFRP

Nonprestressed reinforcement used for the construction of the double tees comprised BRFP with an epoxy resin matrix. The fibers were produced from basalt rock through a melting process. Due to their fairly recent commercial availability, their use is not currently addressed by ACI Committee 440.

Characterization tests were performed according to ACI 440.3R guidelines[18] following the methods currently used for other FRP reinforcement. **Table 2** gives the results of those tests.

Unlike a steel bar, the tensile strength of FRP bars varies with their diameter while the longitudinal modulus does not change appreciably. This phenomenon is primarily due to the effects of shear lag as the matrix transfers stresses from outer fibers to inner fibers within the bar.[19]

Concrete

A self-consolidating concrete (SCC) with specified compressive strength of 8000 psi (55 MPa) was used. The measured air content and spread of the fresh concrete were respectively 1.0% and 25 in. (635 mm). **Table 3** gives the average compressive strengths, measured at different times. The compressive test results were used to compute the tensile strength of the concrete and its modulus of elasticity at different stages. ACI's *Building Code Requirements for Structural Concrete (ACI 318-14) and Commentary (ACI 318-R14)*[20] correlation formulas and the Florida DOT aggregate characterization factor were used.

Design

The pedestrian bridge design takes into account existing guides and technical reports on the use of FRP reinforcement in concrete.[15,19,21] This section focuses on the structural details of the prestressed double tees.

Table 3. Mechanical properties of self-consolidating concrete

	24 hours (one sample)	7 days (three samples)	28 days (three samples)	75 years (analytical)
Compressive strength, psi	5307	7335	8068	8668
Tensile strength, psi	546	642	674	698
Modulus of elasticity, ksi	3599	4232	4438	4600

Note: 1 psi = 6.895 kPa; 1 ksi = 6.895 MPa.

The design of concrete elements prestressed with CFRP is generally based on the assumptions traditionally adopted for concrete prestressed with steel. Of particular interest are the brittle nature of CFRP strands, their long-term behavior under imposed deformations, and their bond-to-concrete properties.[23] Whereas steel tendons are typically stressed up to 85% of their yield stress f_{sy}, allowable stresses in FRP tendons are limited to a significantly lower percentage of their design ultimate strength f_{pu} to prevent possible rupture. According to ACI 440.4R, the recommended maximum jacking stress and maximum stress after the release of CFRP tendons should not exceed 65% and 60% of their design strength, respectively. Conversely, JSCE set these limits to 80% and 70% of the guaranteed strength rather than design strength.

Figure 1 shows a diagram of the pedestrian bridge, including the two double-tee girders (DT1 and DT2), the pile caps, the concrete curb, and the location of the cast-in-place concrete piles. The two juxtaposed girders, nominally identical, are simply supported on a 66 ft (20 m) clear span, resulting in a span width of 14 ft 3 in. (4.34 m).

The bridge is designed to remain uncracked under a distributed live load of 100 lb/ft^2 (4.8 kN/m^2) over its 75-year service life.[22] This load includes dead weights and results in a maximum service moment demand of 947 kip-ft (1280 kN-m) for each of the girders. This corresponds to an ultimate bending demand of 1266 kip-ft (1716 kN-m) and an ultimate shear demand of 76.7 kip (341 kN).

Details

Figure 2 shows the cross section of girder DT1 completed with concrete topping and curbs, and **Fig. 3** shows the top view of the precast concrete element only. The total depth of the precast concrete section is 30 in. (790 mm) with a flange thickness of 4 in. (100 mm).

The total width of the flange is 85¼ in. (2165 mm), and the total length of the girders is 68 ft 8 in. (20.9 m). The thickness of each stem is 7¼ in. (184 mm) at the top and 6 in. (150 mm) at the bottom. Each stem of the double tees includes nine seven-wire CFRP tendons tensioned with an initial prestressing force of 41.25 kip (183.5 kN) per strand before losses. Hence, a total jacking force of 743 kip (3300 kN) with a 10.7 in. (272 mm) eccentricity was applied to each of the double tees.

In addition to the prestressed CFRP tendons, a no. 8 (25M) BFRP bar was positioned at the top and bottom of each stem. The additional nonprestressed reinforcement consists of two preassembled reinforcing meshes made of interwoven BFRP bars. The first mesh acts as longitudinal (no. 4 [13M] at 6 in. [150 mm]) and transverse reinforcement (no. 4 at 6 in.) in the flange. The second mesh (no. 3 [10M] at 6 in. in both directions) was placed on both sides of the CFRP with the aim of reinforcing the transfer length region of the stems. Last, no. 4 BFRP continuous closed stirrups were partially embedded on one side of the flange of both double tees at the time of precasting to serve as transverse reinforcement for the concrete curbs.

The deck was completed on-site with a 3 in. (75 mm) topping and a 14 × 14 in. (360 × 360 mm) curb on the two sides, both cast with a 4000 psi (28 MPa) specified strength concrete. The topping embeds an additional preassembled reinforcing mesh made of interwoven no. 3 (10M) BFRP bars at 8 in. (200 mm) in both the longitudinal and transverse directions.

Material stresses and double-tee capacity

Table 4 shows the total force applied at jacking and the corresponding losses due to elastic shortening of concrete. The prestressing forces imposed intentionally exceeded the threshold suggested by ACI 440.4R while satisfying JSCE requirements. A stress corresponding to 75% of the CFRP design strength (68% of the CFRP guaranteed strength) was therefore applied on each strand at jacking with the purpose of better exploiting the mechanical properties of CFRP tendons.

Table 4 also gives the prestressing force applied if using steel strands according to current practice.[15]

The order of prestressing to be achieved using the two different materials is within a 10% difference, and due to the higher stiffness, the elastic losses due to concrete shortening are slightly higher when steel strands are used rather than CFRP strands (Table 4).

The nominal flexural capacity of the girders was calculated using the specified values of material properties and the

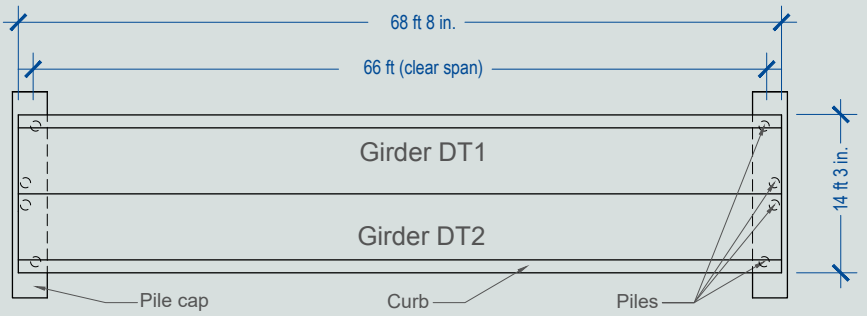

Figure 1. Diagram of the pedestrian bridge. Note: 1 in. = 25.4 mm; 1 ft = 0.305 m.

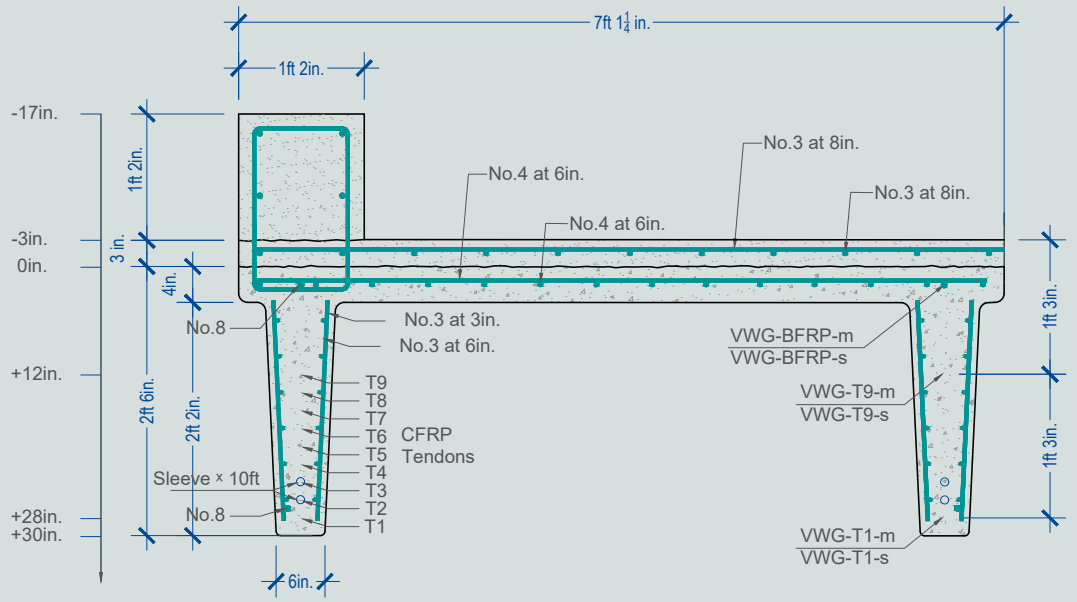

Figure 2. Cross section of the double tee with concrete topping and curb. Note: BFRP = basalt-fiber-reinforced polymer; CFRP = carbon-fiber-reinforced polymer; VWG = vibrating wire gauge. No. 3 = 10M; no. 4 = 13M; no. 8 = 25M; 1 in. = 25.4 mm; 1 ft = 0.305 m.

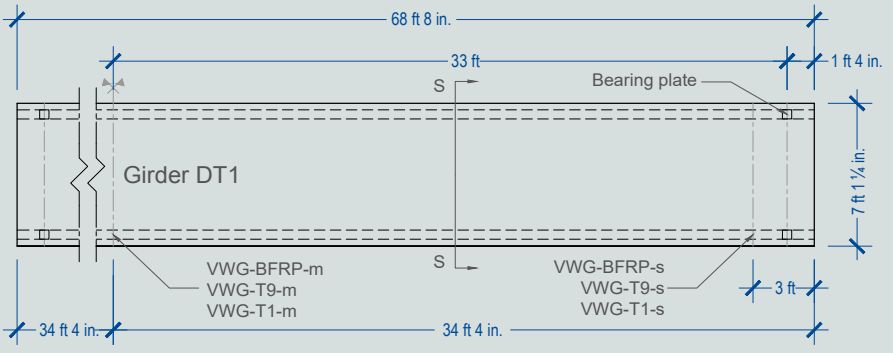

Figure 3. Plan view of the double-tee girder DT1. Note: BFRP = basalt-fiber-reinforced polymer; VWG = vibrating wire gauge. 1 in. = 25.4 mm; 1 ft = 0.305 m.

Table 4. Jacking forces, elastic losses, and forces after transfer

Material	Jacking forces		Elastic losses		Forces after transfer	
	Stress	Load, kip	Percentage	Load, kip	Stress	Load, kip
Carbon-fiber-composite cable (1 × 7)	$0.75f_{pu}$	743	5.7	42	$0.70f_{pu}$	689
Steel (1 × 7)	$0.85f_{sy}$	834	9.3	78	$0.77f_{sy}$	756

Note: f_{pu} = carbon-fiber-reinforced polymer tendon design strength; f_{sy} = steel yield stress. 1 kip = 4.448 kN.

full section of the girders after the concrete topping casting. As previously specified, the environmental reduction factor C_E was adopted to account for long-term exposure to environmental loads. A step-by-step analytical procedure based on the model proposed by Naaman[24] was adopted to compute concrete creep and shrinkage.

Equation (1) was used to calculate the CFRP relaxation losses after a 75-year service life. The resulting nominal flexural capacity and cracking moment of the single double tee, including the concrete topping and curb, at the 75-year service life were 2306 and 1050 kip-ft (3127 and 1424 kN-m), respectively.

Table 5 shows the resulting computed values of stresses in all materials at different phases of the girder's life. The depth axis points downward, and its origin is fixed on the girder top (Fig. 2). Compressive stresses are considered to be negative, whereas tensile stresses are positive.

The double tee loaded by its self-weight was considered at 1-day life (after the tendon's releasing and demolding phases were completed) and 28-day life (fully developed concrete strength). The double tees were installed 126 days after casting, and the completed girder with topping was service loaded at the 154-day life (with the additional 28 days corresponding to the full development of topping concrete strength) and 75-year life.

ACI 440.4R[14] recommends strength reduction factors of 0.85 for tension-controlled behavior when the CFRP tendon strain is above 0.005 and 0.65 for compression-controlled behavior when the net tendon strain is below 0.002. The section lies in the transition zone: the strength reduction factor, computed as a function of the net strain in the furthest tendon at failure, is 0.82. Further discussion of flexural resistance factors for the design of concrete structures prestressed with CFRP is provided by Kim and Nickle[25] and Forouzannia et al.[26]

The factored flexural capacity of each girder, complete with concrete topping and curb, is 1899 kip-ft (2575 kN-m), a value exceeding the design demand at ultimate.

Construction

The precast concrete double-tee girders were constructed and instrumented using a casting bed and prestressing equipment available for conventionally prestressed girders. The tendons and the prefabricated meshes were handled without the aid of mechanical equipment. All the reinforcement was installed and secured before the tensioning took place. Because the concrete elements were precast in line, the tensioning was applied concurrently to the two girders.

Instrumentation

To monitor the strains during the entire service life of the bridge and measure the effective strains and transfer lengths during construction, girder DT1 was instrumented

Table 5. Computed values of stresses at different phases

Location	Depth, in.	Girder only (under self-weight)		Girder with concrete topping (under service loads)	
		1 day, ksi	28 days, ksi	154 days, ksi	75 years, ksi
Curbs (reinforced concrete)	-1	n/a	n/a	-2.4	-2.4
Topping (reinforced concrete)	-3	n/a	n/a	-1.6	-1.6
Double-tee top (prestressed concrete)	0	-0.5	-0.5	-1.4	-1.4
Tendon T9 (carbon-fiber-reinforced polymer)	12	220.6	216.2	214.0	211.7
Tendon T1 (carbon-fiber-reinforced polymer)	28	216.0	209.7	211.9	208.9
Double-tee bottom (prestressed concrete)	30	-2.1	-2.0	0.4	0.4

Note: n/a = not applicable. 1 in. = 24.5 mm; 1 ksi = 6.895 MPa.

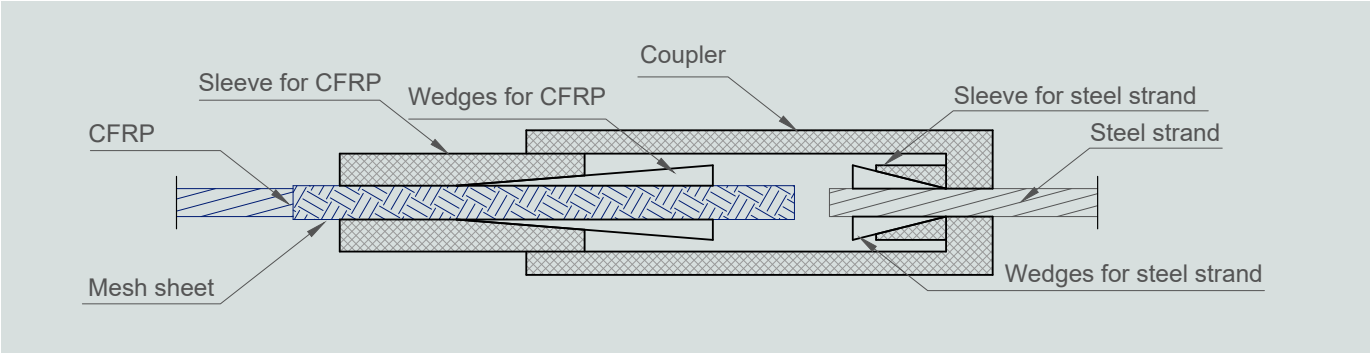

Figure 4. Carbon-fiber-composite cable and steel strand coupling anchorage system. Note: CFRP = carbon-fiber-reinforced polymer.

with six vibrating wire gauges (VWGs): four installed on the CFRP tendons and two installed on the BFRP reinforcement. The top tendon T9 and the bottom tendon T1 of a selected stem of girder DT1 were instrumented with two gauges at the double-tee midspan (VWG-T9-m and VWG-T9-s) and two more at about 3 ft (0.9 m) from one of the end sections (VWG-T9-s and VWG-T9-s) (Fig. 2 and 3). VWG-BFRP-m and VWG3-BFRP-s were installed on the BFRP longitudinal reinforcement similarly to the gauges on the monitored stem, at the double-tee midspan and at 3 ft from the same end section, respectively.

Tensioning

CFRP is a brittle material, sensitive to shocks caused by hard and sharp objects. Consequently, applying a tension force to CFRP using a mechanical device is a process that requires particular care.

The conventional tensioning apparatus available at the precasting plant, consisting of a hydraulic jack powered by a pump, is used to pull the steel cables. To facilitate use of this same device to pretension the CFRP strands, they were attached to steel strand using a proprietary mechanical anchorage system. This facilitated the pulling of the strands without causing localized damage to the CFRP.

The device (**Fig. 4**) consists of two anchoring systems based on sleeves and wedges (one for CFRP and one for steel), connected by a coupler. Each CFRP tendon was equipped with a mesh sheet and a braided grip to protect it from damage (Fig. 4). Table 1 gives the steel cable properties. The tensioning force of 41.25 kip (183.5 kN) was measured by means of a calibrated pressure transducer, and applied stresses were verified by measuring the cable elongation as well as detecting the strains in the instrumented tendons. After the tensioning was completed, SCC was placed.

Releasing

Steel strands are normally flame cut using a torch to take advantage of the gradual energy release caused by the elevated temperature, which lowers the yielding point of steel. This process cannot be adopted for FRP tendons because they would be degraded by the heat. Rather, FRP tendons must be severed using a high-speed grinder. For this reason, the tension was released at the two ends of the prestressing bed by cutting the steel rather than the CFRP strands. After the end release, the CFRP strands between the two double tees were carefully cut using a grinder. The prestress release took place 24 hours after casting. At that time, the measured concrete compressive strength was 5307 psi (36.59 MPa). Following these operations, the girders were successively demolded.

Strain monitoring

Table 6 lists the strain measurements detected on the CFRP tendons at the instrumented sections after the tensioning phases (0 hours), after the concrete placement (6 hours), after the release of prestressing forces (24 hours), and after the complete curing of the prestressed concrete girders (26 days). The first strain loss deals with the pretensioning apparatus settlement (CFRP-and-steel anchorage system). The second loss is due to the elastic shortening of concrete at the time of the release and the overnight CFRP relaxation. The third loss is caused by concrete creep and CFRP relaxation during the 26 days of curing. The average between the experimental values measured at the top tendon T9 and bottom tendon T1 is the strain at the centroid of the tendons. Table 6 gives the analytical prediction of the strains at the girder midspan section with respect to the centroids of the tendons. The computed values of losses due to CFRP tendon relaxation were two orders of magnitude lower than that due to the creep effects in concrete. For this reason, the numerical values provided in Table 6 are not visibly affected by the relaxation contribution of the CFRP tendons.

The strains measured at the double-tee girder midspan (VWG-T9-m and VWG-T1-m) confirm the prescribed values at jacking and are in agreement with the theoretical

Table 6. Strains in carbon-fiber-reinforced polymer tendons

Location	Measured/computed quantity	Tensioning (0 hours), %	Casting (6 hours), %	Releasing (24 hours), %	26 days, %
Midspan	VWG-T1-m	1.06	1.03	1.01	0.94
	VWG-T9-m	1.01	0.95	0.93	0.90
	Average	1.04	0.99	0.97	0.92
	Analytical (centroid)	1.05	n/a	0.97	0.93
3 ft (0.9 m) from end	VWG-T1-s	0.95	0.92	0.54	0.17
	VWG-T9-s	0.99	0.93	0.98	1.07
	Average	0.97	0.93	0.76	0.62

Note: n/a = not applicable; VWG = vibrating wire gauge.

prediction of losses. The strains detected at 3 ft (0.9 m) from the end section (VWG-T9-s and VWG-T1-s) show a partial loss of bond of the bottom tendon T1. This phenomenon was not expected because both VWGs were meant to be installed beyond the development-length zone of the tendons. However, the sleeves installed on tendons T2 and T3 at the two ends of the double tees (Fig. 2) may have negatively affected the bond behavior of tendon T1.

Load test

As shown in **Fig. 5**, the flexural response under service conditions, a static load test was conducted on the instrumented girder DT1 at the precasting plant before its installation on-site. The test, conducted according to a three-point loading scheme over the 66 ft (20 m) effective span, took place 26 days after casting.

Test arrangement

The test load magnitude was designed to avoid concrete cracking. The analytical procedure was refined to account for the actual properties of the concrete used and the progressive gain of strength and stiffness due to aging (Table 3). The original design requires the girders to remain uncracked under service loads, and the test was run accordingly. The effects of the 100 lb/ft^2 (4.8 kN/m^2) distributed live load on the fully completed bridge (double tees with topping and curbs) were considered to back-calculate the point load that would produce the same effect on the double tees only. This resulted in a 27 kip (120 kN) test load in addition to the self-weight, which was supposed to produce a maximum moment of 809 kip-ft (1100 kN-m) on the single double tee. The test condition corresponds to the 85% of the double-tee cracking moment, defined as that which forces the concrete from the initial compressive stress of -1840 psi (-12.7 MPa) to the cracking tensile stress of 673 psi (4.64 MPa), computed per ACI 318-14 recommendations and accounting for concrete strength gain over time.

Four rectangular hollow steel tubes placed over prismatic concrete elements were used as supports (**Fig. 6**). A soft wood interface was provided between the supports and the girder bearing plates to help the leveling process and prevent stress concentration during the test. Three rectangular concrete blocks, each of them weighing 9 kip (40 kN), were used to apply the intended load by means of a crane (Fig. 5).

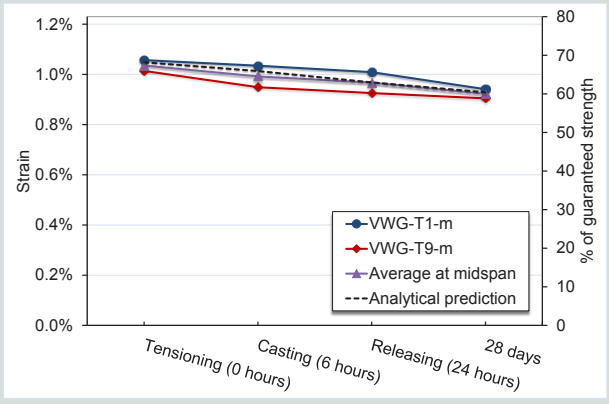

Figure 5. Strains in carbon-fiber-reinforced polymer tendons at midspan. Note: 1 ft = 0.305 m.

Figure 6. Double-tee girder loading phase, dial gauges, and supports.

The double-tee girder displacements were monitored using 10 analogic dial gauges installed on the two stems (**Fig. 7**). Dial gauges 1, 2, 3, and 4 were used to monitor the supports settlement. Dial gauges 7 and 8 were intended to measure the double-tee deflection at midspan, and dial gauges 5, 6, 9, and 10 were positioned symmetrically at the quarter spans (Fig. 7).

The 27 kip (120 kN) total load was applied in three steps. After applying one block, the second and third concrete blocks were positioned on the double-tee girder then removed and permanently repositioned on the girder midspan. The total load was sustained over a 24-hour period. The loading and unloading phases required about two hours each. The dial gauge measurements were monitored at each load step.

Results and discussion

Figure 8 shows the midspan and quarter-span deflections compared with experimental load values obtained during the 24-hour loading cycle. The analytical prediction of the midspan deflection-load curve is also shown.

The girder exhibited the elastic performance expected under loading corresponding to service conditions with no visible cracking. Due to the sustained 27 kip (120 kN) load, additional deformations (mainly resulting from concrete creep) were observed during the 24-hour monitoring. The observed elastic deflection at 27 kip and additional deflection after 24 hours of sustained loading were consistent with analytical predictions (errors of +2% and +12%, respectively) (**Table 7**). However, the experimental value of the residual deflection immediately after the load removal is considerably higher than predicted (error of +30%), probably because elastic recovery is not instantaneous.

Similar considerations apply to the measurement performed on the girder camber. The predicted analytical values of the camber deviate only +6% and +5% from the values measured before and after the performance of the load test, respectively, with the experimental absolute values being slightly higher than expected (Table 7).

Table 7. Deflection at midspan and girder camber (absolute values)

	Experimental values, in.	Analytical prediction, in.	Error, %
Elastic deflection (27 kip, 0 hours)	1.076	1.093	+2
Additional deflection (27 kip, 24 hours)	0.116	0.104	+12
Residual deflection (0 kip, 24 hours)	0.135	0.104	+30
Initial camber (26 days)	1.957	1.843	-6
Posttest camber (27 days)	1.823	1.738	-5

Note: 1 in. = 24.5 mm; 1 kip = 4.448 kN.

Figure 9 shows the deflection profiles of the girder at the different loading phases and the corresponding analytical curves. Also in this case, the theoretical modeling appears fully capable of describing the behavior of the structural element at the monitored sections and for different levels of loads.

Finally, **Fig. 10** illustrates the measured strain profile at the girder midspan section and the analytical prediction of elastic strains corresponding to the 27 kip (120 kN) loading. The experimental data detected on the tendons are in satisfactory agreement with the theoretical values and show the expected linearity of the strains along the midspan cross section. The strains measured on bottom tendon T1

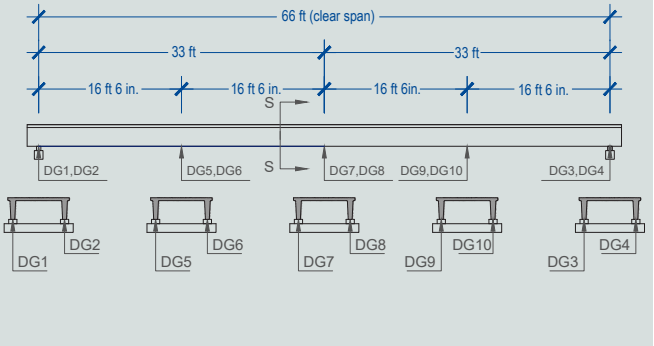

Figure 7. Dial gauge locations. Note: DG = dial gauge. 1 in. = 25.4 mm; 1 ft = 0.305 m.

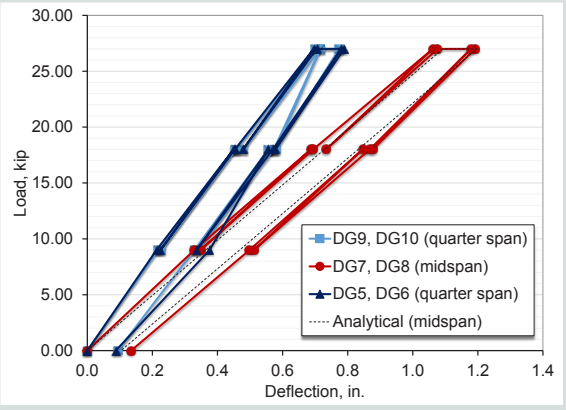

Figure 8. Load-deflection curves. Note: DG = dial gauge. 1 in. = 25.4 mm; 1 kip = 4.448 kN.

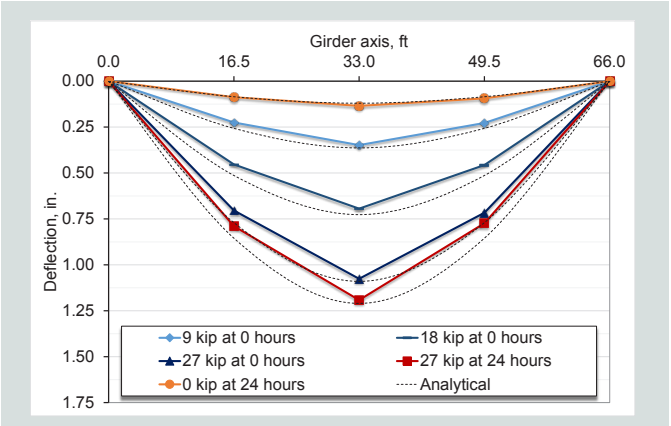

Figure 9. Deflection profile along the beam axis. Note: 1 in. = 25.4 mm; 1 ft = 0.305 m; 1 kip = 4.448 kN.

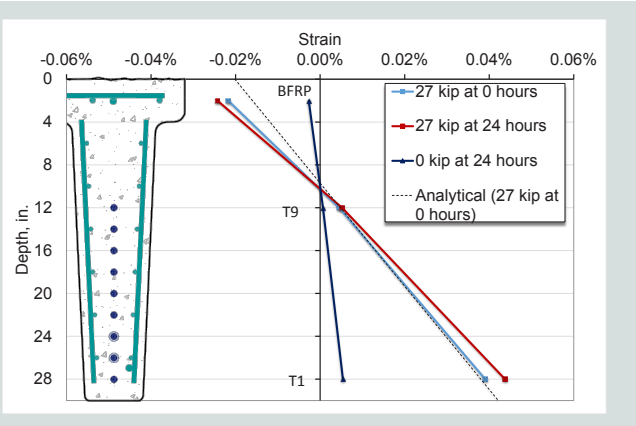

Figure 10. Measured strain profile at girder DT1 midspan. Note: 1 in. = 25.4 mm; 1 kip = 4.448 kN.

and the top tendon T9 differ by +3% and -6%, respectively, from the analytical predictions. Only the strain measured on the BFRP mesh is considerably higher than the predicted analytical value (+36%).

Conclusion

In this study, assumptions traditionally used for steel-prestressed concrete were adopted for the design of thin-walled double-tee CFRP-prestressed concrete sections, leading to construction details similar to those of steel-prestressed concrete structures to resist the same loads. Some differences arose with respect to the tensioning procedure. A mechanical anchoring system able to facilitate the pulling of the strands without damaging them allowed the CFRP tendons to be attached to prestressed concrete steel cables and, consequently, a conventional tensioning apparatus. In this respect, the great flexibility of the method was recognized in view of the limited use of FRP strands and unavailability of tensioning equipment in precasting plants.

CFRP tendons showed mechanical efficiency comparable to typical steel strands due to a higher guaranteed load, elastic behavior up to failure, and a lower elastic modulus, resulting in reduced losses. Increasing the level of pretension over the current ACI 440.4R limit and using 0.6 in. (15 mm) diameter CFRP tendons in the thin stems of double tees are the key factors for exploiting the properties of such materials, which, if properly employed, may lead to levels of performance even higher than those achievable by steel-prestressed concrete structures. Although beyond the scope of this study, this goal could be achieved by improving manufacturing and quality control techniques, resulting in a higher guaranteed load and the possibility of exploiting a larger percentage of the tendons' ultimate strength.

Monitoring tendon strain in the construction phase and the elastic response of the double tee to the static load test, along with the long-term measurement of camber and deflection, showed evidence of the reliability of the analytical predictions. All calculations were performed based on established theories and mechanical models and demonstrated that the implementation of CFRP tendons may not require additional design efforts by practitioners.

Strains and deformations observed under sustained load appear to be largely dominated by the rheological behavior of concrete. As expected, the relaxation of CFRP tendons does not seem to affect the deformation of the girders. Additional tests are planned to monitor the bridge's performance over time and are intended to confirm the short-term conclusions.

This study shows that CFRP prestressing technology can be successfully employed on thin-walled concrete sections without corrosion drawbacks. Performances can be compared to those of steel reinforcement and can be pushed beyond the limits imposed by current guidelines.

Acknowledgments

The research component of this project was funded under the aegises of the University Transportation Center for Research on Concrete Applications for Sustainable Transportation (RE-CAST), the National Science Foundation Industry/University Cooperative Research Center for the Integration of Composites into Infrastructure (CICI), and the Infravation project SEACON. The University of Miami research team also included Thomas Cadenazzi, Carlos Noel Morales, Omid Gooranorimi, Guillermo Claure, and Francisco J. De Caso y Basalo. Saverio Spadea's research visit to the University of Miami was funded by the J. William Fulbright Foreign Scholarship Board.

Project credits go to OHL Arellano Construction Co., the general contractor; Anzac Contractors, the bridge subcontractor; Brill Rodriguez Salas & Associates Inc., the engineer of record; the University of Miami, the architectural design and designated engineer; the University of Miami Structures and Materials Laboratory, the research coordinator; Coreslab Structures, the double-tee

fabricator; Tokyo Rope/Tokyo Rope USA Inc., the CFRP manufacturer; No Rust Rebar Inc., the BFRP manufacturer; Hughes Brothers Inc., the GFRP manufacturer; Titan America, the concrete supplier; and MAPEI, the surface products supplier.

References

1. Ahmad, S. 2003. "Reinforcement Corrosion in Concrete Structures, Its Monitoring and Service Life Prediction—A Review." *Cement and Concrete Composites* 25 (4–5): 459–71.

2. Bertolini, L., B. Elsener, P. Pedeferri, E. Redaelli, and R. Polder. 2014. *Corrosion of Steel in Concrete: Prevention, Diagnosis, Repair*. Weinheim, Germany: Wiley-VCH.

3. Nanni, A., A. De Luca, and H. J. Zadeh. 2014. *Reinforced Concrete with FRP Bars: Mechanics and Design*. Boca Raton, FL: CRC Press.

4. Jamshaid, H., and R. Mishra. 2016. "A Green Material from Rock: Basalt Fiber—A Review." *The Journal of The Textile Institute* 107 (7): 923–937. https://doi.org/10.1080/00405000.2015.1071940.

5. Fiore, V., T. Scalici, G. Di Bella, and A. Valenza. 2015. "A Review on Basalt Fibre and Its Composites." *Composites Part B: Engineering* 74: 74–94.

6. Nanni, A., G. Claure, F. J. De Caso y Basalo, and O. Gooranorimi. 2016. "Concrete and Composites Pedestrian Bridge." *Concrete International* 38 (11): 57–63.

7. Ushijima, K., T. Enomoto, N. Kose, and Y. Yamamoto. 2016. "Field Deployment of Carbon-Fiber-Reinforced Polymer in Bridge Applications." *PCI Journal* 61 (5): 29–36.

8. Spadea, S., J. Orr, Y. Yang, and A. Nanni. 2017. "Wound FRP Shear Reinforcement for Concrete Structures." *Journal of Composites for Construction*. 21 (5). https://doi.org/10.1061/(ASCE)CC.1943-5614.0000807.

9. Grace, N. F., T. Enomoto, S. Sachidanandan, and S. Puravankara. 2006. "Use of CFRP/CFCC Reinforcement in Prestressed Concrete Box-Beam Bridges." *ACI Structural Journal* 103 (1): 123–32.

10. Grace, N. F., K. D. Patki, E. Soliman, and J. Q. Hanson. 2001. "Flexural Behavior of Side-by-Side Box-Beam Bridges: A Comparative Study." *PCI Journal* 56 (3): 94–112.

11. Grace, N., T. Enomoto, P. Baah, and M. Bebawy. 2012. "Flexural Behavior of CFRP Precast Prestressed Decked Bulb T-Beams." *Journal of Composites for Construction* 16 (3): 225–34.

12. Grace, N., K. Ushijima, P. Baah, and M. Bebawy. 2013. "Flexural Behavior of a Carbon Fiber-Reinforced Polymer Prestressed Decked Bulb T-Beam Bridge System." *Journal of Composites for Construction* 17 (4): 497–506.

13. Grace, N., K. Ushijima, V. Matsagar, and C. Wu. 2013. "Performance of AASHTO-Type Bridge Model Prestressed with Carbon Fiber-Reinforced Polymer Reinforcement." *ACI Structural Journal* 110 (3): 491–501.

14. Grace, N. F. 2000. "Transfer Length of CFRP/CFCC Strands for Double-T Girders." *PCI Journal* 45 (5): 110–26.

15. ACI (American Concrete Institute) Committee 440. 2004. *Prestressing Concrete Structures with FRP Tendons*. Reapproved 2011. ACI 440.4R. Farmington Hills, MI: ACI.

16. JSCE (Japan Society of Civil Engineers). 1997. "Design Guidelines of FRP Reinforced Concrete Building Structures." Concrete engineering series no. 23. Tokyo, Japan: JSCE.

17. Tokyo Rope Manufacturing Co. Ltd. 2014. "Report for Long Term Relaxation of CFCC 1 × 7 15.2ϕ." Tokyo, Japan: Tokyo Rope Manufacturing Co. Ltd.

18. ACI Committee 440. 2012. *Guide Test Methods for Fiber-Reinforced Polymers (FRPs) for Reinforcing or Strengthening Concrete Structures*. ACI 440.3R. Farmington Hills, MI: ACI.

19. ACI Committee 440. 2015. *Guide for the Design and Construction of Structural Concrete Reinforced with Fiber-Reinforced Polymer Bars*. ACI 440.1R. Farmington Hills, MI: ACI.

20. ACI Committee 318. 2014. *Building Code Requirements for Structural Concrete (ACI 318-14) and Commentary (ACI 318-R14)*. Farmington Hills, MI: ACI.

21. AASHTO (American Association of State Highway and Transportation Officials). 2009. *AASHTO LRFD Bridge Design Guide Specifications for GFRP-Reinforced Concrete Bridge Decks and Traffic Railings*. Washington, DC: AASHTO.

22. AASHTO. 2014. *AASHTO LRFD Bridge Design Specifications.* Washington, DC: AASHTO.

23. Burke, C. R., and C. W. Dolan. 2001. "Flexural Design of Prestressed Concrete Beams Using FRP Tendons." *PCI Journal* 46 (2): 76–87.

24. Naaman, A. E. 2012. *Prestressed Concrete Analysis and Design: Fundamentals*. 3rd ed. Ann Arbor, MI: Techno Press 3000.

25. Kim, Y. J., and R. W. Nickle. 2016. "Strength Reduction Factors for Fiber-Reinforced Polymer-Prestressed Concrete Bridges in Flexure." *ACI Structural Journal* 113 (5): 1043–52.

26. Forouzannia, F., B. Gencturk, M. Dawood, and A. Belarbi. 2016. "Calibration of Flexural Resistance Factors for Load and Resistance Factor Design of Concrete Bridge Girders Prestressed with Carbon Fiber-Reinforced Polymers." *Journal of Composites for Construction* 20 (2). https://doi.org/10.1061/(ASCE)CC.1943-5614.0000613.

Notation

C_E = environmental reduction factor

f_{pu} = carbon-fiber-reinforced polymer tendon design strength

f^*_{pu} = carbon-fiber-reinforced polymer tendon guaranteed ultimate strength

f_{sy} = steel yield stress

T = time

Y = relaxation rate

About the authors

Saverio Spadea, PhD, is a lecturer (assistant professor) in structural engineering design at the University of Dundee in the United Kingdom. During the 2015 through 2016 academic year, he visited the University of Miami in Coral Gables, Fla., for six months as a J. William Fulbright Scholar.

Marco Rossini is pursuing a PhD in civil engineering at the University of Miami. He completed his MS in structural engineering and his bachelor's degree in civil engineering at Politecnico di Milano in Italy.

Antonio Nanni, FACI, FASCE, is a professor in and chair of the Department of Civil, Architectural and Environmental Engineering at the University of Miami. He serves as chair of ACI Committee 549 and Subcommittee 562-E and a voting member of ACI Committees 437, 440, and 562.

Abstract

This paper deals with the design philosophy and the flexural performance under service loads of the precast, prestressed concrete girders constituting the deck of a recently constructed pedestrian bridge. This simple structure combines innovative materials and novel composite manufacturing technologies to ensure that degradation due to steel corrosion does not undermine the longevity of the bridge.

The two girders, cast in the shape of double tees with shortened flange overhangs, were prestressed with 0.6 in. (15 mm) diameter, seven-wire carbon-fiber-reinforced polymer (CFRP) tendons and reinforced with basalt-fiber-reinforced polymer bars. Despite the complexity inherent in its tensioning, CFRP strand has already been used for other prestressed or post-tensioned applications, but never before in large diameters for the fabrication of structural elements with thin cross sections. The selected percentage of the guaranteed capacity of the CFRP tendons applied at jacking was, for the first time, higher than the 65% limit imposed by ACI 440.4R-04 guidelines.

A load test was performed at the precasting yard with concentrated loads corresponding to service conditions, with the tested girder remaining uncracked. The strains measured in the reinforcement and the detected deflections of the girder showed agreement with the analytical predictions. CFRP prestressing technology can be used successfully in thin-walled concrete sections beyond the limits suggested by current guidelines and without significant technological drawbacks.

Keywords

Basalt fiber, BFRP, bridge, carbon-fiber-reinforced polymer, CFRP, double tee, fiber-reinforced polymer, flexural performance, FRP, girder, prestressing, tensioning.

Review policy

This paper was reviewed in accordance with the Precast/Prestressed Concrete Institute's peer-review process.

Reader comments

Please address reader comments to journal@pci.org or Precast/Prestressed Concrete Institute, c/o *PCI Journal*, 200 W. Adams St., Suite 2100, Chicago, IL 60606.